Factors Affecting Climate Sensitivity in Global Coupled Models

GERALD A. MEEHL, WARREN M. WASHINGTON, JULIE M. ARBLASTER, AND AIXUE HU

National Center for Atmospheric Research, Boulder, Colorado*

(Manuscript received 9 June 2003, in final form 16 September 2003)

ABSTRACT

Four global coupled climate models with different combinations of atmosphere, ocean, land surface, and sea ice components are compared in idealized forcing (1% CO_2 increase) experiments. The four models are the Climate System Model (CSM), the Parallel Climate Model (PCM), the PCM/CSM Transition Model (PCTM), and the Community Climate System Model (CCSM). The hypothesis is posed that models with similar atmospheric model components should show a similar globally averaged dynamically coupled response to increasing CO_2 in spite of different ocean, sea ice, and land formulations. Conversely, models with different atmospheric components should be most different in terms of the coupled globally averaged response. The two models with the same atmosphere and sea ice but different ocean components (PCM and PCTM) have the most similar response to increasing CO_2, followed closely by CSM with comparable atmosphere and different ocean and sea ice from either PCM or PCTM. The fourth model, CCSM, has a different response from the other three and, in particular, is different from PCTM in spite of having the same ocean and sea ice but different atmospheric model component. These results support the hypothesis that, to a greater degree than the other components, the atmospheric model ''manages'' the relevant global feedbacks including sea ice albedo, water vapor, and clouds. The atmospheric model also affects the meridional overturning circulation in the ocean, as well as the ocean heat uptake characteristics. This is due to changes in surface fluxes of heat and freshwater that affect surface density in the ocean. For global sensitivity measures, the ocean, sea ice, and land surface play secondary roles, even though differences in these components can be important for regional climate changes.

1. Introduction

Compilations of global coupled climate models run with increased CO_2 show a range of response of globally averaged surface air temperature (Cubasch et al. 2001). The reasons for these differences in response remain unclear since all the models have different components and combinations of parameterizations. It has been demonstrated that interchanging model components in a systematic fashion so that the influence of the different components can be elucidated has proved useful (Washington and Meehl 1991; Meehl et al. 2000a,b; Guilyardi et al. 2004, manuscript submitted to *J. Climate*, hereafter GUI). The latter study showed that, for ENSO frequency characteristics, the atmosphere component was most important, while for ENSO amplitude, the ocean component played a greater role. Here we will use a similar approach in comparing four models, with some components in common and changes in others, to address the issue of characteristics of globally averaged surface air temperature response, commonly used as a measure of climate sensitivity. We will quantify three feedbacks typically cited as important for climate sensitivity (e.g., Stocker et al. 2001), namely, sea ice/albedo, water vapor, and cloud. Though these feedbacks do not operate independently (e.g., Schneider et al. 1999), we will evaluate them diagnostically to provide an indication of the relative size of their respective contributions to global climate sensitivity and response. Additionally, important aspects of climate sensitivity involve geographic patterns of various feedbacks that are related to differences in the various model components (e.g., Meehl et al. 2000b; Boer and Yu 2003a,b). Here we identify and quantify the various forcings and responses as global averages, and acknowledge that regional patterns of the changes could depend on the details of the different components included in the coupled models.

Following the results of Guilyardi et al. and considering that the most commonly cited uncertainties in climate models involve clouds and convection, both contained in the atmosphere component, we hypothesize that the relevant feedbacks involved with coupled climate model sensitivity at the global scale are ''managed'' mostly by the atmospheric model component. Thus the ocean, sea ice, and land surface components may be secondary to the first-order global feedbacks involved with the climate system response to increasing

* The National Center for Atmospheric Research is sponsored by the National Science Foundation.

Corresponding author address: Dr. Gerald A. Meehl, National Center for Atmospheric Research, P.O. Box 3000, Boulder, CO 80307. E-mail: meehl@ncar.ucar.edu

TABLE 1. Description of components in the four global coupled climate models. Note that the CCSM version here is CCSM2.0. The subsequent recently released version, CCSM3.0, has different characteristics.

	CSM	PCM	PCTM	CCSM
Atmosphere	CCM3.2 T42, 18 Levels	CCM3.2 T42, 18 Levels	CCM3.2 T42, 18 Levels	CAM T42, 26 Levels
Ocean	NCOM, 2° 45L, GM, KPP	POP, ⅔° (½° in equatorial Tropics), 32L, biharmonic diffusion, Pacanowski and Philander (1981) mixing	POP, 1° (½° in equatorial Tropics), 40L, GM, KPP	POP, 1° (½° in equatorial Tropics), 40L, GM, KPP
Sea ice	Cavitating fluid and thermodynamic	Dynamic (EVP) and thermodynamic	Dynamic (EVP) and thermodynamic	Dynamic (EVP) and thermodynamic
Land surface	LSM	LSM	LSM	CLM

CO_2. Consequently, models with similar atmospheric model components should show similar response to increasing CO_2 in spite of different ocean, sea ice, and land surface formulations. Additionally, models with different atmosphere components should be most different in terms of globally averaged response.

Section 2 includes a brief summary of the four models. Section 3 presents results for the transient climate response of the four models globally and geographically, followed by section 4, which addresses the various feedbacks at work in the models and their respective contributions to the transient climate response, and section 5 contains an analysis of ocean heat uptake processes. Section 6 includes a summary of results and conclusions.

2. Description of models

A summary of the characteristics of the four models compared in this study appears in Table 1. We briefly elaborate on those features below.

The Climate System Model (CSM) uses a version of CCM3.2 for the atmosphere component at T42 and 18 levels in the vertical (Kiehl et al. 1998). The ocean is the National Center for Atmospheric Research (NCAR) Ocean Model (NCOM) with 2° resolution and 45 levels, with Gent–McWilliams (GM) mixing and K Profile Parameterization (KPP; Gent et al. 1998). The sea ice component is a cavitating fluid (Washington and Meehl 1989), and land surface is the Land Surface Model (LSM) described by Bonan (1998).

The Parallel Climate Model (PCM) uses the same version of CCM3.2 for the atmosphere as in CSM. The ocean is different from CSM and uses the Parallel Ocean Program (POP) with 2/3° resolution going down to 1/2° in the equatorial Tropics, with 32 levels in the vertical. Physics includes biharmonic diffusion and Pacanowski and Philander (1981) vertical mixing. The sea ice component includes dynamic [elastic–viscous–plastic (EVP)] and thermodynamic components. The land surface component is the same as in CSM. The PCM is described in detail in Washington et al. (2000). El Niño amplitude is close to observed in this model (Meehl et al. 2001).

The PCM/CSM Transition Model (PCTM) includes elements of PCM and CSM (the same atmosphere and land surface), but with the same ocean and sea ice components (Gent et al. 2002) as in the Community Climate System Model (CCSM) described below.[1]

The CCSM uses a different atmospheric model than the other three, the Community Atmospheric Model (CAM) at T42 resolution and 26 levels in the vertical (June 2002 release version of CCSM2.0; see online at http://www.ccsm.ucar.edu/models/ccsm2.0/). Major improvements were made to the radiation and convection schemes, and there is an inclusion of a prognostic cloud liquid water scheme. The ocean is a version of POP with 1° resolution increasing to 1/2° in the equatorial Tropics and with 40 levels in the vertical. Physics include GM and KPP. Sea ice is EVP and thermodynamic. The land component is the Community Land Model (CLM). Differences from the LSM include 10 layers for soil temperature and soil water, a multilayer snowpack, and a new formulation of ground and vegetation fluxes (Bonan et al. 2002).

We intend to focus in particular on the responses of the two models with the same atmosphere and sea ice and different ocean, the PCM and PCTM, and compare those with another model with the same atmosphere but different ocean and sea ice, the CSM. Finally, we will pay close attention to the two models with different atmosphere components but the same ocean and sea ice, the PCTM and CCSM. In general, if our hypothesis

[1] Note use of the term ''the same'' when referring to various model components in this paper means that the model versions are scientifically the same. No two model versions are identical bit for bit usually due to small logistical changes in the model code or, in the case of sea ice between PCM and PCTM, a different grid. However, these changes do not affect the scientific results and allow for intercomparison across model versions. Additionally, version numbers of models are omitted in this paper for simplicity, but it should be noted that CSM is also referred to as CSM1.0, and PCM can be called PCM1. The CAM is also called CAM2, and for CCSM the version number is CCSM2.0. Version CCSM3.0, released in late 2003, has different response characteristics and will be documented in subsequent papers.

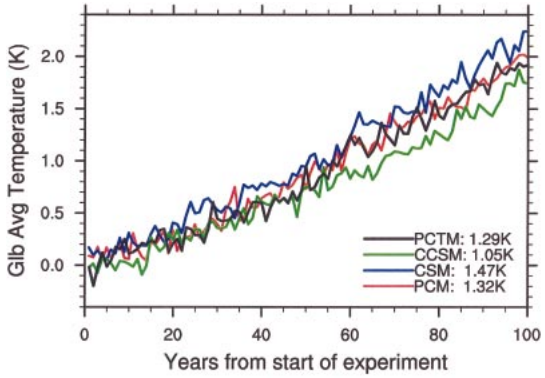

FIG. 1. Time series of globally averaged surface air temperature anomalies (cf. the respective control runs) from the four models for a 1% compound increase of CO_2, with CO_2 doubling around year 70. Transient climate response for the four models is shown in the lower right-hand corner.

holds, the three models with the same atmosphere components but various different ocean and sea ice components, CSM, PCM, and PCTM, will be more comparable in their globally averaged responses than the CCSM with a different atmosphere component compared to the other three.

3. Transient climate response

A usual starting point for comparing different models' sensitivity in transient climate experiments is the transient climate response (TCR) (Cubasch et al. 2001). TCR is defined as the globally averaged surface air temperature difference for the 20-yr period around the time of CO_2 doubling minus the control run. This can be compared to the definition of climate sensitivity as the globally averaged surface air temperature difference for a doubled CO_2 experiment run to equilibrium with a nondynamic slab ocean coupled to the atmosphere. Effective climate sensitivity as defined in Cubasch et al. is the time-evolving climate system response and provides an estimate of the strength of the feedbacks at a specific time. The equilibrium sensitivity equals effective sensitivity with $2 \times CO_2$ forcing. Thus, climate sensitivity, effective climate sensitivity, and TCR are not equivalent. For example, the climate sensitivity for CCM3 (the atmosphere in CSM, PCM, and PCTM) is 2.1°C, while for CAM it is 2.2°C, while TCR values for the four coupled models containing the atmospheric versions are quite different as noted below. This points to the important roles of feedbacks and ocean heat uptake that are the subjects of this paper.

Figure 1a shows the time series of globally averaged surface air temperature and the TCR for the four different models. CO_2 doubles around year 70, and the 20-yr average from years 61–80 is calculated for each model and 50-yr averages from the respective control runs are used for the differences. The nature of the individual model responses is not distinguishable until about year 50. After that it becomes evident that the CSM warms the most, the CCSM the least, and PCM and PCTM are in between. The CSM is the most sensitive of the four with a TCR of 1.47°C. The PCM and PCTM are comparable with TCR of 1.32° and 1.29°C, respectively. The CCSM has the lowest TCR value of 1.05°C. Thus the models with the same atmospheric component, PCM, PCTM, and CSM, have TCR values that are closer than CCSM. For example, PCM and PCTM have responses that are very close. If the TCR values for those two models are averaged and compared to CSM and CCSM, the CSM is 13% larger while the CCSM is 20% less sensitive. Thus the effects on the CSM TCR from different ocean and sea ice components are greater than just changing the ocean component from PCM to PCTM. But the change in atmospheric component in CCSM produces the greatest impact on TCR. As noted above, the equilibrium climate sensitivities of CCSM (2.2°C), PCM, PCTM, and CSM (2.1°C for the latter three) are comparable, but the respective TCR values from the four models vary more. This points to the vital role of feedbacks and ocean heat uptake in the dynamically coupled climate system response to increasing CO_2.

However, these are single realizations, and it could be argued that the spread among the models is due only to differences of response that could be expected from variability among ensemble members. To give an idea of the variability of the TCR in a single model, a five-member ensemble of 1 percent per year CO_2 increase runs was performed with the PCM. These particular five ensemble members were run to the time of CO_2 doubling at year 70. The last 20 years of these simulations are evaluated for intraensemble variability compared to corresponding periods of the respective control runs. The intraensemble standard deviation of TCR for these PCM simulations is 0.03°C, indicating that natural variability and different initial conditions can introduce variability of TCR in a five-member ensemble that is comparable to the difference between the PCM and PCTM, which have TCR values of 1.32° and 1.29°C, respectively. This indicates their responses are indistinguishable from the standard deviation of responses in a multimember ensemble. For the model with the same atmosphere but a different ocean, the CSM, the TCR of 1.47°C is around 5% different from the PCM and PCTM, indicating that the change in ocean and sea ice components make a difference to the simulation that is outside the expected variability of a multimember ensemble, but less than two standard deviations of the interannual standard deviation from 100-yr control runs of PCM (0.09°), PCTM (0.09°), and CSM (0.10°C).

However, for the model with the significantly different atmosphere, the CCSM, the TCR is 1.05°C, roughly from 20% to 35% lower than the other three models, and well outside several intraensemble standard deviations of the PCM (0.03°C), as well as the natural variability standard deviation from either of the other three

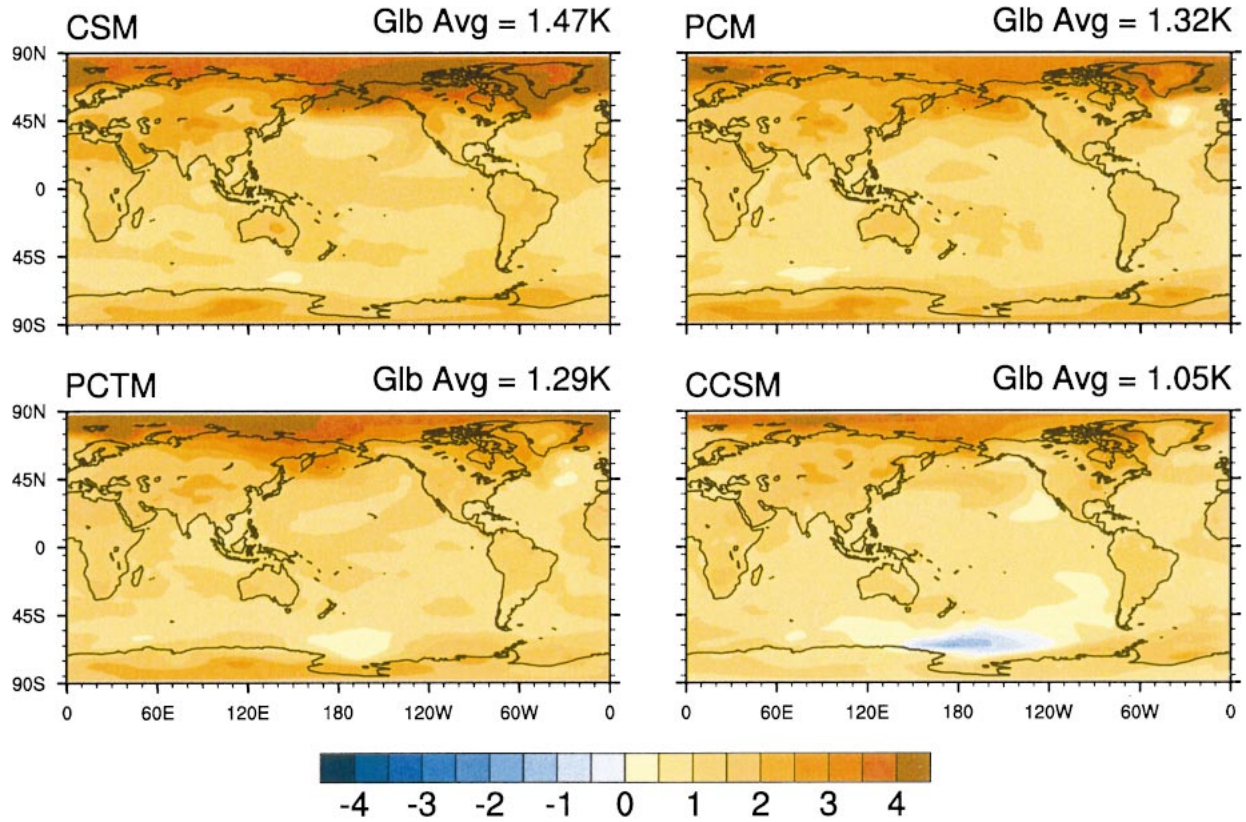

FIG. 2. Reference height (surface air) temperature differences (°C), 20-yr average around the time of CO_2 doubling, years 61–80, minus respective control run averages for the four models for (a) CSM, (b) PCM, (c) PCTM, and (d) CCSM.

models mentioned above or the CCSM itself (0.08°C). Most notable is the fact that the atmosphere (CAM) is different in the CCSM compared to the other three models (CCM3.2). Additionally, the model closest in configuration to CCSM, the PCTM, which has the same ocean and sea ice schemes but different atmosphere, has a TCR greater than the CCSM by 0.24°C, over two standard deviations of natural variability in any or the four models, and well over eight standard deviations of the intraensemble standard deviation from the PCM. Thus, if the ocean and sea ice were the main contributors to sensitivity, one would expect the PCTM and CCSM to be more similar in terms of response since they both share the same ocean and sea ice components. However, the PCTM (TCR of 1.29°C) has a 20% greater TCR compared to the CCSM (TCR of 1.05°C). Though the land surface components are different in these two models, we will show below that the relevant feedbacks depend more on the atmosphere component.

TABLE 2. Zonal mean warming divided by global mean warming for different latitude bands.

	CSM	PCM	PCTM	CCSM
North of 45°N	2.06	1.85	1.76	1.79
45°N–45°S	0.82	0.89	0.87	0.90
South of 45°S	0.79	0.84	0.84	0.68

The geographic patterns of surface air temperature change for the four models are shown in Fig. 2. All show the characteristic pattern, seen in other models (e.g., Cubasch et al. 2001), of greater warming at high northern latitudes and over continents and less warming in the North Atlantic and southern oceans. The size of the regional anomalies is roughly proportional to the TCR for the respective models. For example, for the latitude bands 45°–90°N, 45°N–45°S, and 45°–90°S, the relative warming is proportional to the globally averaged values. For 45°–90°N, CSM, the most sensitive model, has the greatest warming at that latitude band, 3.0°, compared to the other models with values of +2.4° (PCM), +2.3°C (PCTM), and +1.9°C (CCSM). The PCM and PCTM, closest together for globally averaged TCR, are also closest together in all three bands, with the PCM values of +2.4°, +1.1°, and +1.2° comparable to the values of +2.3°, +1.1°, and +1.1 (°C) in PCTM.

Meanwhile, the CCSM, with the lowest value of TCR, has the lowest values in each of the latitude bands compared to the other models with values of +1.9, +0.9, and +0.7 (°C), respectively. The ratios of surface temperature warming in those bands to the globally averaged temperature are given in Table 2 and show that they are roughly comparable among all the models. If the regional anomalies were exactly proportional to

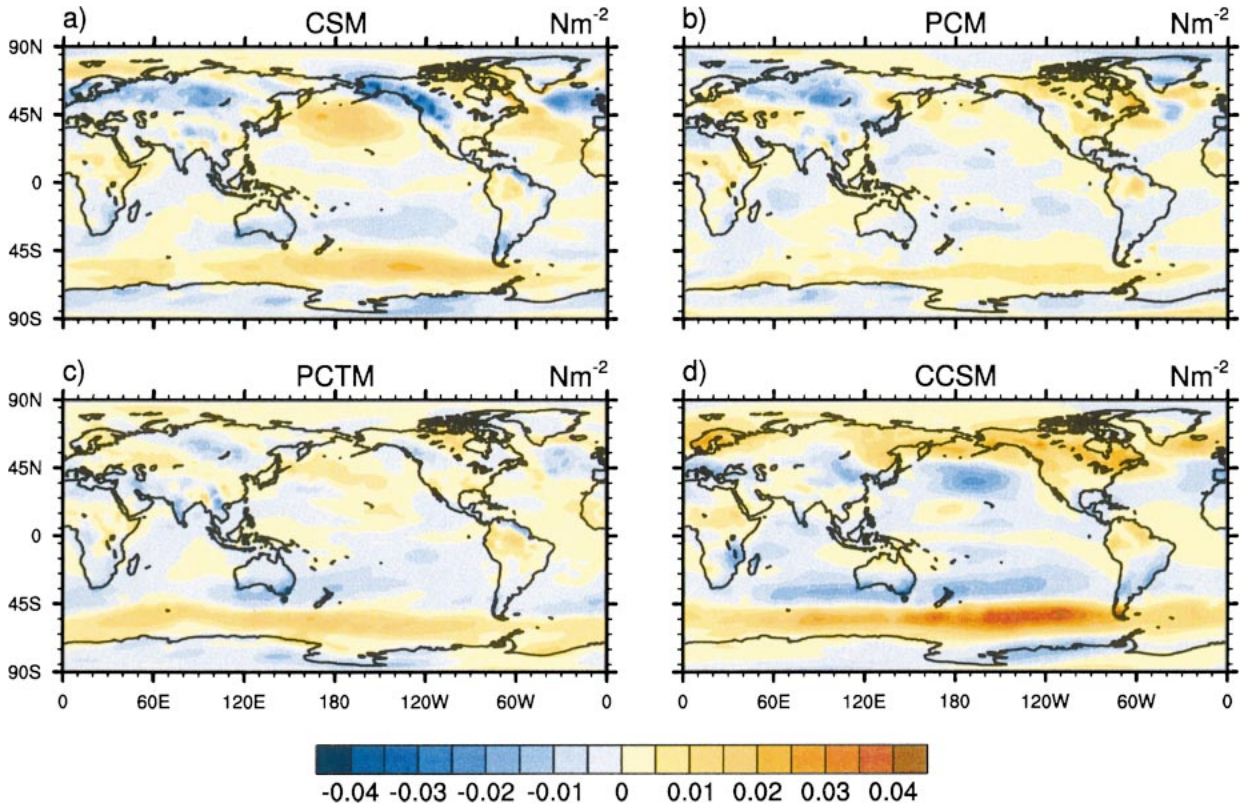

FIG. 3. As in Fig. 2 except for *u*-component surface wind stress (N m^{-2}).

TCR, the regional ratios in Table 2 would not have any variation among the models. However, they vary between about 15% and 19% for the high northern and high southern latitudes, respectively. This indicates, as noted in the discussion for Fig. 2, that feedbacks can vary the regional contributions to the globally averaged response somewhat. Further discussion of the numbers in Table 2 will be given later in regards to effects on ocean heat uptake.

Of particular regional interest is the near-zero warming in the PCM and PCTM in the North Atlantic in Figs. 2b and 2c, respectively, and the patch of warming less than +0.5°C in PCTM in the South Pacific Ocean in Fig. 2c, and negative temperature anomalies in that same region the CCSM in Fig. 2d. For the former, Dai et al. (2004, manuscript submitted to *J. Climate*) show that a change in wind forcing in the atmosphere component common to PCM and PCTM shifts the course of the Gulf Stream to the south. Thus, warm water from the Gulf Stream near 45°N is replaced by cooler water from the north, producing little relative warming in the difference. That there is a similar pattern of response in the PCM and PCTM in the North Atlantic suggests that this is related to the atmospheric forcing since both PCM and PCTM share identical atmospheric models.

For the southern Pacific Ocean, a similar effect is taking place, but related to the ocean component common between PCTM and CCSM. Figure 3 shows changes in the *u* component wind stress for the four models. Deepening of the circumpolar trough seen in most other models (Cubasch et al. 2001) also occurs in these four models, and is indicated by positive wind stress differences near 45°–55°S (stronger westerlies). The greatest strengthening of the southern westerlies is in CCSM with increases around 0.05 N m^{-2} in the South Pacific, compared to increases half that amplitude in PCTM in that region and even smaller in PCM. This increases Ekman transport more in CCSM and, in the ocean model component common to PCTM and CCSM, shifts the position of the Antarctic Circumpolar Current to the north when CO_2 is increased (Fig. 4). This shift is signified by relatively cooler water from the south being located near 55°S, producing the low amplitude warming in PCTM and the negative surface temperature anomalies in CCSM in that region. Thus, details of the regional response can depend more closely on the component models. But the changes in regional surface air temperature noted above for PCM, PCTM, and CCSM do not appreciably change the globally averaged response since the areas covered by these temperature anomalies are small. Additionally, it was shown above that the ratio of the warming in the various latitude bands to the globally averaged warming is comparable among the four models, with values around 2°C at high northern latitudes, and closer to 1°C elsewhere. Thus the amplitude of the global response involves the sum

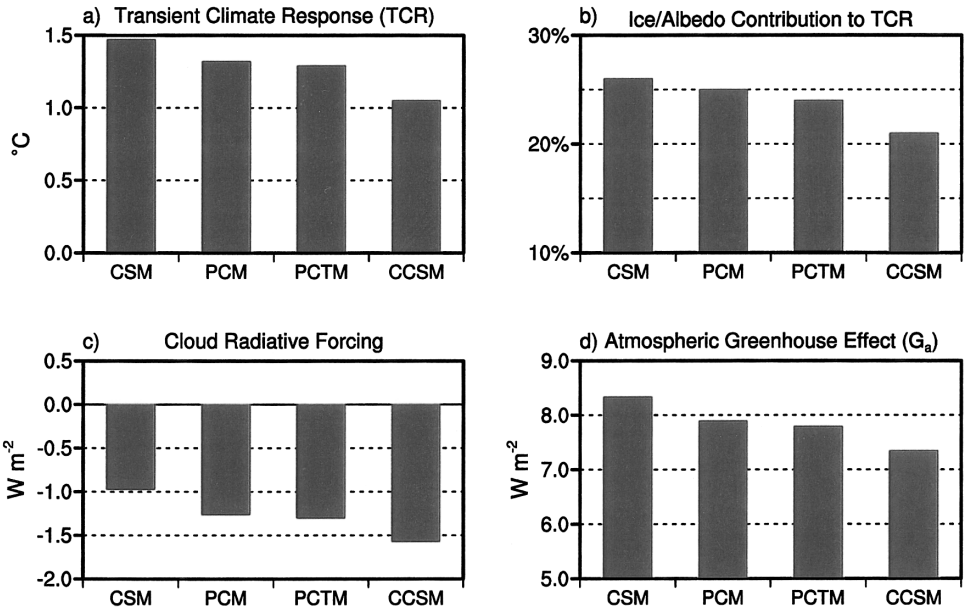

FIG. 4. (a) Globally averaged surface air temperature difference (°C) around the time of CO_2 doubling for years 61–80 minus control (transient climate response or TCR); (b) Sea ice–albedo feedback contribution (%) to TCR from the four models; (c) as in (a) except for cloud radiative forcing (W m^{-2}); (d) as in (a) except for atmospheric greenhouse effect (W m^{-2}).

of the entire global climate system and cannot be easily attributed to processes specific to one latitude band.

4. Feedbacks

In order to address the hypothesis in the introduction, the strategy for the feedback intercomparison is to quantify three globally averaged feedbacks: 1) sea ice/albedo, 2) water vapor, and 3) cloud. The effect of all these feedbacks and others acting in the models can be calculated as the feedback parameter (λ) as in Raper et al. (2002) in the following equation:

$$\Delta Q = \lambda \Delta T + \Delta F, \quad (1)$$

where ΔQ is the radiative forcing for a doubling of CO_2, ΔT is the transient climate response or TCR defined as the globally averaged surface air temperature change at the time of CO_2 doubling in a 1 percent per year transient CO_2 increase experiment, and ΔF is the net heat flux into the surface [see further discussion in Cubasch et al. (2001) and Raper et al. (2002)]. In effect, this means that the radiative forcing from a doubling of CO_2 must either be manifested as an increase in temperature or an increase in heat flux into the surface, with the feedback factor that can amplify the response. Thus, the larger the λ, the smaller the size of the feedbacks in the climate system.

TABLE 3. Feedback parameter λ for the four models (small λ = large feedbacks).

	CSM	PCM	PCTM	CCSM
λ	1.80	2.00	2.10	2.48

Values of λ (unit: W m^{-2} °C^{-1}) are given in Table 3 for the four models. The models with the most similar atmosphere components, CSM (1.80), PCM (2.00), PCTM (2.10), have the most similar values of λ (all within 10% of each other), and thus comparably sized global feedbacks. However, the model with the most different atmosphere, the CCSM, has a value of λ of 2.48, about 15%–30% larger than the other three. This indicates that globally averaged feedbacks are more strongly related to the atmospheric model component in these global climate models. As we did above for TCR, we can average the values of λ for the two most similar models, PCM and PCTM, which yields a value of 2.05, and note that the CSM value of λ is 12% less, while CCSM is 21% greater.

Figure 4 summarizes globally averaged measures related to the feedbacks that affect the climate system response to increased CO_2. Figure 4a shows the TCR values discussed above. Figure 4b includes results from a calculation that estimates the ice–albedo feedback contribution to the TCR after Dickinson et al. (1987) and Meehl et al. (2001). It is assumed that changes in top-of-atmosphere net clear-sky solar radiation for increased CO_2 are mostly related to differences in ice and snow cover. Using change in net clear-sky solar radiation for ΔF in Eq. (1), recalculating the contribution to λ, and then computing ΔT, the percent change in TCR with and without ice and snow changes is plotted in Fig. 4b. The CSM, PCM, and PCTM all have comparable chang-

es of TCR when ice and snow albedo feedback effects are excluded, and range from 24% to 26%. The CSM has quite a different sea ice component compared to PCM and PCTM, yet all three still yield a similar implied sea ice–albedo feedback contribution to global warming. However, the CCSM has a lower sea ice–albedo contribution of about 20%. Even though CCSM has the same ocean and sea ice formulations as in PCTM, yet has quite a different atmospheric component. The intraensemble standard deviation from the five-member PCM ensemble for this measure is 0.7%. Thus the CSM, PCM, and PCTM are all around plus or minus one intraensemble standard deviation, while the CCSM lies well outside the two standard deviation range. This result is somewhat surprising given the fact that, in particular, the CSM has a much different and simplified sea ice scheme (cavitating fluid) compared to the other three models (with EVP and thermodynamic schemes). However, the contribution from the CSM is proportional to the globally averaged TCR in Fig. 4a and not appreciably different from the PCM or PCTM. That the CCSM is quite different from PCTM in spite of essentially the same sea ice scheme provides further evidence supporting the importance of the feedbacks being managed by the atmosphere components that are different in those two models.

Early concepts of climate sensitivity related base state temperature in the control run to the size of the response to increased CO_2, with a colder base state associated with greater sensitivity (e.g., Spelman and Manabe 1984). This was mainly attributed to ice–albedo feedback effects wherein a colder model would have more sea ice area that could react to warming with a stronger ice–albedo feedback, and thus produce even greater warming as a consequence. However, subsequent studies (e.g., Meehl and Washington 1990) showed that this simple relationship becomes less straightforward when the sea ice scheme becomes more complicated. For the models here, the base state temperature of the least sensitive model (lowest TCR), the CCSM, is the warmest at 287.5 K, and the PCM and PCTM have somewhat colder base state temperatures (285.4 and 286.4 K, respectively) and greater TCR. So for these models, the relationship between base state temperature and climate response holds. However, the most responsive model, the CSM, with a base state temperature of 285.8 K does not have the coldest base state as would be expected from the simple relationship noted above. In fact, the PCM has the coldest base state temperature. Additionally the base state temperature does not have much to do with the magnitudes of the sea ice–albedo feedbacks in Fig. 4b. The CSM also has the most different sea ice scheme from the other models suggesting that, consistent with Meehl and Washington (1990), variants of sea ice schemes (and other factors) complicate the relationship between base state temperature and climate response seen in some of the earlier models.

An indication of cloud feedback in the models is given by the change in total cloud radiative forcing (the sum of cloud shortwave and cloud longwave radiative forcing), and results for this calculation are plotted in Fig. 4c. All the models show negative differences in total cloud radiative forcing with doubled CO_2, with values ranging from -0.97 for CSM, to -1.57 W m^{-2} for CCSM, indicating that a negative cloud feedback is operating in all the models. That is, the changes in cloud feedback in all the model versions are acting to reduce global warming, and are likely to be one of the reasons for the relatively low sensitivity of these models in comparison to other state-of-the-art global coupled GCMs (Cubasch et al. 2001). For this measure, CCSM again is the most different from the other three, with the largest negative cloud radiative forcing of -1.57 W m^{-2}. This can be compared to smaller values of -1.30 W m^{-2} for PCTM, -1.26 W m^{-2} for PCM, and a somewhat lower value for CSM of -0.97 W m^{-2}. The ranking among the models of the cloud feedback values in Fig. 4c again reflect the TCR values in Fig. 4a, with the model with the most different atmospheric component, CCSM, having the largest negative cloud radiative forcing. The intraensemble standard deviation for the five-member PCM ensemble for this measure is 0.03 W m^{-2}. Interannual standard deviations from 100-yr control runs for the four models range from 0.17 W m^{-2} for CSM to 0.23 W m^{-2} for PCM. As before for TCR and sea ice/albedo, PCM and PCTM are within one standard deviation of each other for both measures. CSM, the most sensitive model, has a significantly smaller negative cloud radiative forcing (23% less than PCM, more than two intraensemble standard deviations, and more than one interannual standard deviation), while CCSM, the least sensitive model, has the largest negative cloud radiative forcing (21% more than PCTM, more than two intraensemble standard deviations and more than one interannual standard deviation). Thus, the two models with the same atmosphere, the PCM and PCTM, have nearly the same changes in cloud radiative forcing. A change in ocean and sea ice reduces the magnitude of the negative cloud radiative forcing in the CSM, while a change in the atmosphere (to CAM in CCSM) increases the magnitude of the negative cloud radiative forcing. This indicates that changes in cloud radiative forcing, and thus cloud feedback, are affected by changes in all components, in particular the atmospheric component between PCTM and CCSM.

Measures of water vapor feedback are somewhat more difficult to obtain in coupled models. One measure is G_a, the atmospheric greenhouse effect (e.g., Ramanathan and Collins 1991), and is defined

$$G_a = \sigma T^4 - \mathrm{OLR}_{\mathrm{tc}}, \tag{2}$$

where σ is the Stephan–Boltzman constant, T is surface temperature, and $\mathrm{OLR}_{\mathrm{tc}}$ is net outgoing clear-sky longwave radiation at the top of the atmosphere. Since all models have the same increase of CO_2, to first-order G_a is then a measure of water vapor effects in the atmo-

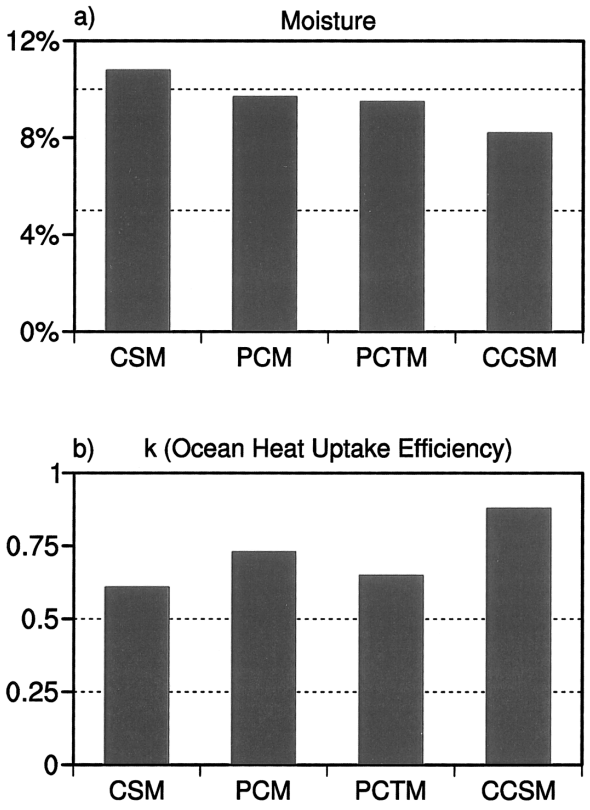

FIG. 5. (a) As in Fig. 4a except for percent change in total column moisture; (b) same as (a) except for changes in ocean heat uptake efficiency.

sphere. Therefore, for these four models, the greater the value of G_a, the larger the water vapor feedback in the system. Figure 4d shows differences of G_a for the four models at the time of CO_2 doubling. Reflecting the TCR values in Fig. 4a, G_a is largest for the model that warms most, the CSM, with a G_a difference of 8.33 W m^{-2}. PCM and PCTM are near each other with values of 7.89 and 7.79 W m^{-2}, respectively, while CCSM has the smallest G_a difference of 7.35 W m^{-2}. Intraensemble standard deviation is 0.09 W m^{-2}, and interannual standard deviations from the control runs range from 0.25 W m^{-2} for PCTM to 0.31 W m^{-2} for PCM. Thus, the CCSM has the smallest water vapor feedback among the four models and is associated with the smallest global warming as indicated from the TCR in Fig. 4a. PCM and PCTM, with the same atmospheric components but different oceans, are within one intraensemble and natural variability standard deviation and are thus statistically indistinguishable from each other. The CSM difference is about 6% larger than PCM, but is greater than one natural variability standard deviation and more than two intraensemble standard deviations from the PCM and PCTM. The CCSM response is nearly 6% less than the PCTM, but is also greater than one natural variability standard deviation and more than two intraensemble standard deviations from the PCM and PCTM. This result is similar to the cloud radiative forcing in the four models in Fig. 4c.

As a check for the G_a calculation as a representation of water vapor feedback, the total moisture content of the atmosphere can be computed for the four models. Presumably greater moisture content should indicate larger water vapor feedback and be consistent with the changes in G_a in Fig. 4d. Figure 5a shows changes in total vertically and globally integrated atmospheric moisture changes for the four models. Consistent with the G_a differences in Fig. 4d, Fig. 5a shows that the CSM has the largest moisture increase of 10.8%, PCM and PCTM are close with 9.7% and 9.5% increases, respectively, while the least sensitive model with the lowest G_a difference in Fig. 4d is the CCSM with a change in total moisture of 8.2%. The intraensemble standard deviation for moisture change is 0.3%.

5. Ocean heat uptake

Since the equilibrium sensitivities among the models are nearly the same but the TCR values are quite different, the role of feedbacks noted above all contribute to the TCR differences. However, feedbacks in the atmosphere are not the whole story for the climate system response to an increase in CO_2. As shown in Eq. (1), the increased energy to the system from an increase in CO_2 either goes into warming the atmosphere with the feedback factor λ, or the energy goes into the ocean as indicated by the change in the net heat flux. As defined by Gregory and Mitchell (1997), ocean heat uptake efficiency is a way to compare the relative amounts of energy going into the ocean among models. Ocean heat uptake efficiency, k, is defined as

$$k = \Delta F/\Delta T, \tag{3}$$

where ΔF is the change in forcing from increased CO_2, and ΔT is the TCR. For the disparate models in the Coupled Model Intercomparison Project (CMIP), Raper et al. (2002) showed that the least sensitive models tend to have the lowest heat uptake efficiency and the most sensitive models usually have the greatest k. Their conclusion was that ocean heat uptake has a compensating effect on the range of TCR in coupled model simulations of global warming compared to the range of equilibrium climate sensitivities from the same models.

Values of k are calculated for the four models under consideration here, and are shown in Fig. 5b. The CCSM has the largest k of 0.88, while the other three are more comparable with values of 0.61 (CSM), 0.73 (PCM), and 0.65 (PCTM). Intraensemble standard deviation for k is 0.15. Therefore, for this measure the CSM, PCM, and PCTM are all within one standard deviation, while the CCSM is greater than one standard deviation away from each of the other three.

Thus, the model that has the lowest TCR here, the CCSM, has the largest ocean heat uptake efficiency, counter to the results of Raper et al. (2002). It may be

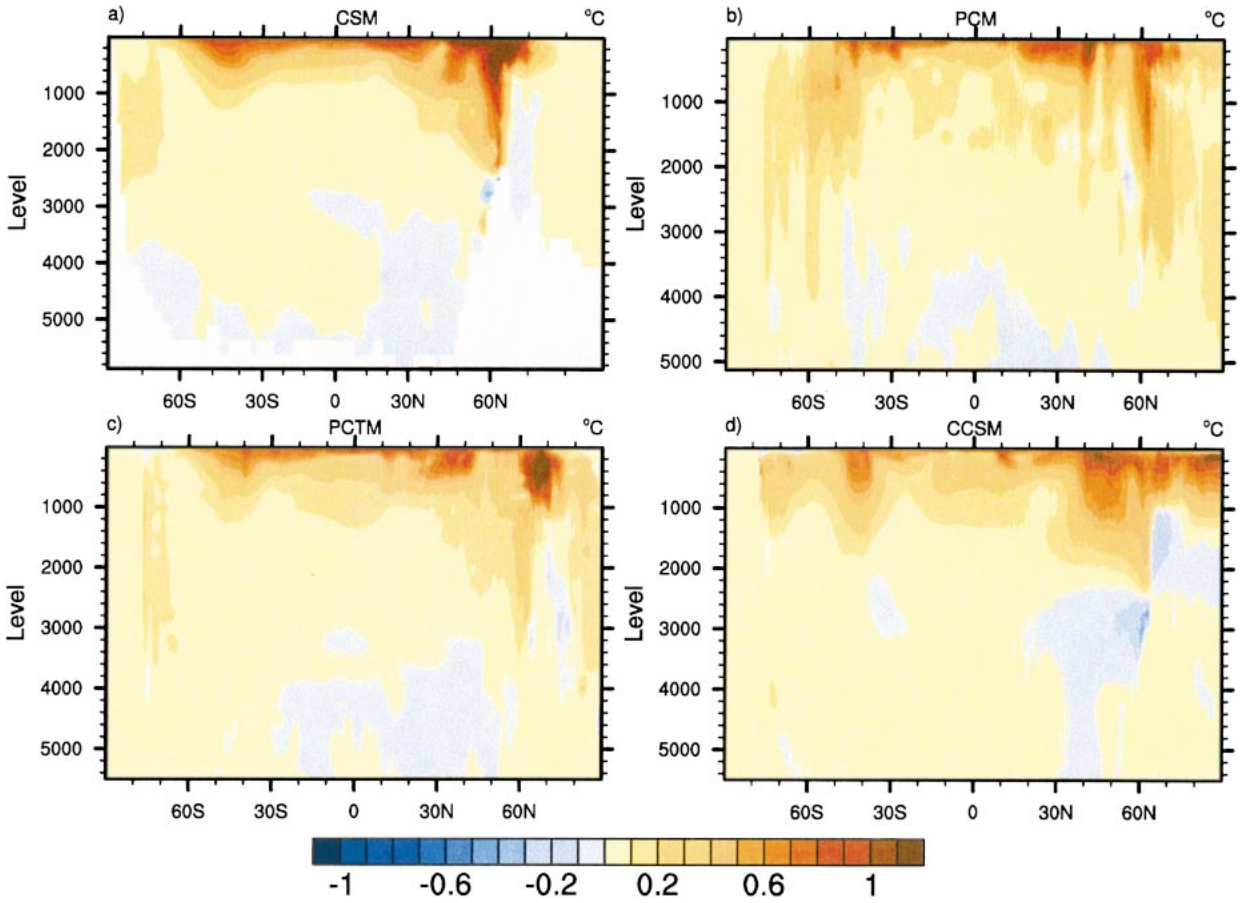

FIG. 6. As in Fig. 2 except for zonal-averaged cross section of ocean temperature differences (°C).

that the range of TCR, narrow for the four models considered here compared to the much broader range in Raper et al., put such ocean responses in the noise level in the larger model context. However, ocean heat uptake processes have received relatively little attention in the past in the climate response literature and deserve further scrutiny here.

As noted above, Raper et al. showed a relationship between k and λ, with small values of λ (high sensitivity) usually associated with large values of k (large ocean heat uptake efficiency). Here, the model with the smallest value of λ (the CCSM with $\lambda = 2.48$) and lowest sensitivity has the largest value of k at 0.88. This is not a unique characteristic of this single CCSM experiment. A subsequent 1% CO_2 increase simulation was performed with the CCSM, and the value of k in that experiement was 0.79, somewhat smaller than the first CCSM simulation, but still considerably larger than the other models in Fig. 5b and greater than one intraensemble standard deviation.

The differences in ocean heat uptake efficiency are evident in the zonal mean ocean temperature differences in Fig. 6. All show warming in the upper 1000 m of the ocean of around a degree Celsius at most latitudes, with greatest positive anomalies near 60°N. The differences in the penetration of heat into the ocean due to a change in the ocean model are seen by comparing PCM (Fig. 6b) with PCTM (Fig. 6c). The greatest amplitude warming in PCM is mostly contained to the upper 200 m, while PCTM warming extends more uniformly down to 1000 m at most latitudes. There is also more heat that penetrates below 2000 m near 60°S in PCM compared to PCTM as indicated by positive temperature differences at those depths. The CSM (Fig. 6a) has the more uniform warming seen in PCTM even though the CSM has a different ocean, but with very little heat penetration north of about 70°N in contrast to the other three models. The CCSM (Fig. 6d) has warming of nearly 1°C down to 500 m at the high latitudes of the Northern Hemisphere, in contrast to the PCTM (with the same ocean but different atmosphere) that has most of its warming in the upper 1000 m near 70°N.

Raper et al. (2002) posed several possible explanations linking k and λ. They noted that increased stability due to warming and freshening of the ocean surface layer with increased CO_2 results in less cold dense water sinking in the North Atlantic, a relative warming at depth at those latitudes (less heat loss from the interior

of the ocean), and consequent greater heat uptake, relatively speaking. Therefore, Raper et al. suggested that a reduction of heat loss at high latitudes from the ocean means more heat uptake by the ocean, a warmer more stable surface layer, and enhanced high-latitude warming of surface air temperatures. They postulate that high-latitude warming could be greater relative to the global mean in models with higher sensitivity. To explore this possibility, Table 2 (as noted earlier) shows results for the four models considered here where the zonal mean surface air temperature warming for three latitude bands (the high latitudes poleward of 45° and the regions from 45°N to 45°S) is divided by the global mean warming (TCR). The most sensitive model, the CSM, has the largest relative proportion of warming north of 45°N at 2.06°, while the least sensitive model, the CCSM, has the smallest relative proportion of warming south of 45°S (0.68°). However the PCTM and CCSM have nearly the same proportion of warming at high northern latitudes and extrapolar latitudes, but have quite different TCR values.

Another possibility posed by Raper et al. is that the increased stability of the ocean due to surface warming could slow down the meridional overturning circulation (MOC) in the ocean, as is known to occur in various other climate models with increased CO_2 (e.g., Cubasch et al. 2001). A reduction of MOC would mean less cold dense water sinking at high latitudes, relatively larger warming in the subsurface, and, consequently, greater ocean heat uptake due to less ventilation of the ocean. Figure 7a shows the values of maximum MOC in the North Atlantic from the four models for the control run, and the difference for the increased CO_2 simulations (Fig. 7b). Interestingly, the model with highest sensitivity, the CSM, actually has a small *increase* in MOC strength with doubled CO_2 (also noted by Gent 2001), while the other less-sensitive models show decreases in MOC. This runs counter to the Raper et al. conclusion that models with greater sensitivity should have a relatively larger *decrease* in MOC. This change in MOC for CSM is associated with large subsurface warming in the sinking region in the North Atlantic noted in Fig. 6a. Gent (2001) indicates that this is due to the North Atlantic surface waters in CSM being warm and becoming more saline. Therefore, the surface density is not significantly affected, the MOC actually slightly strengthens, and it carries the warmer and denser water down to warm the subsurface without a weakening in the MOC.

Meanwhile, by changing only the atmospheric model, the control run value of MOC in CCSM decreases by 36% from 25.16 Sv (Sv $\equiv 10^6$ m^3 s^{-1}) in PCTM to 16.02 Sv in CCSM. This is a dramatic illustration of the effect of the atmosphere on the ocean and provides insight into the different response characteristics of the MOC. Figure 8a shows the change in net surface heat flux for CCSM minus PCTM. The change in the atmospheric model from PCTM to CCSM has increased

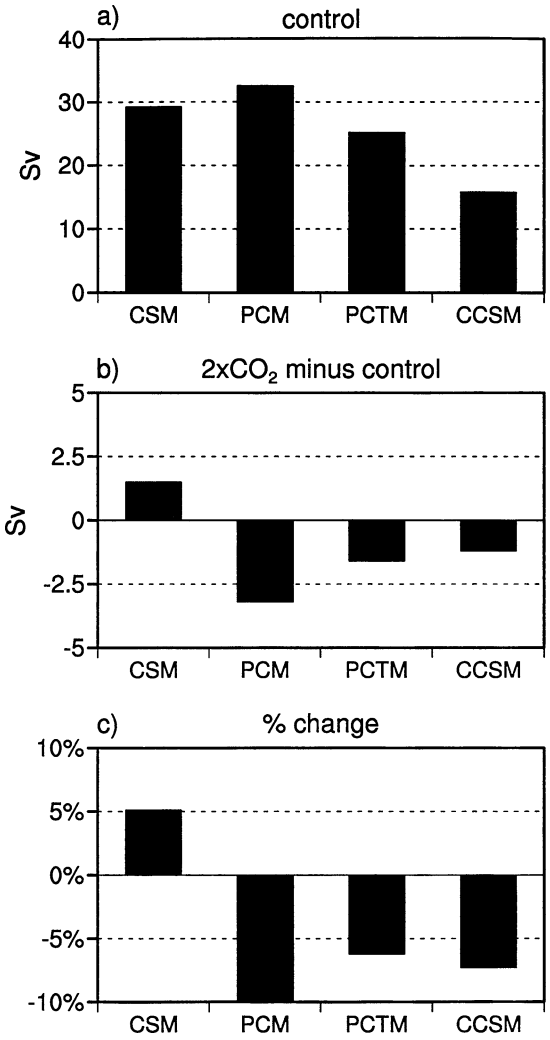

FIG. 7. North Atlantic Ocean meridional overturning circulation (a) maximum values from the control run for the four models (Sv), (b) differences of MOC around the time of CO_2 doubling, years 61–80, minus respective control run averages for the four models (Sv), and (c) percent change in MOC for a doubling of CO_2 [values in (b) divided by values in (a)].

the net surface heat flux into the North Atlantic south and east of Iceland from about 20 to 30 W m^{-2}. There is also a warmer ocean surface in the North Atlantic and Greenland Sea of about 0.5°–1.0°C (Fig. 8b). However, the change in evaporation minus precipitation is positive in the North Atlantic region surrounding Iceland in Fig. 8c, though the values are small (order of several tenths of a meter per year). This would contribute to an increase of density and stronger MOC. However, the relative changes in temperature and salinity in the North Atlantic must be viewed in combination since, together, they produce changes in density that affect the MOC (e.g., Hu et al. 2004). The fact that the MOC is reduced in CCSM compared to PCTM indicates that the stabilizing increases in surface temperature win out over the contributions to increased salinity by pos-

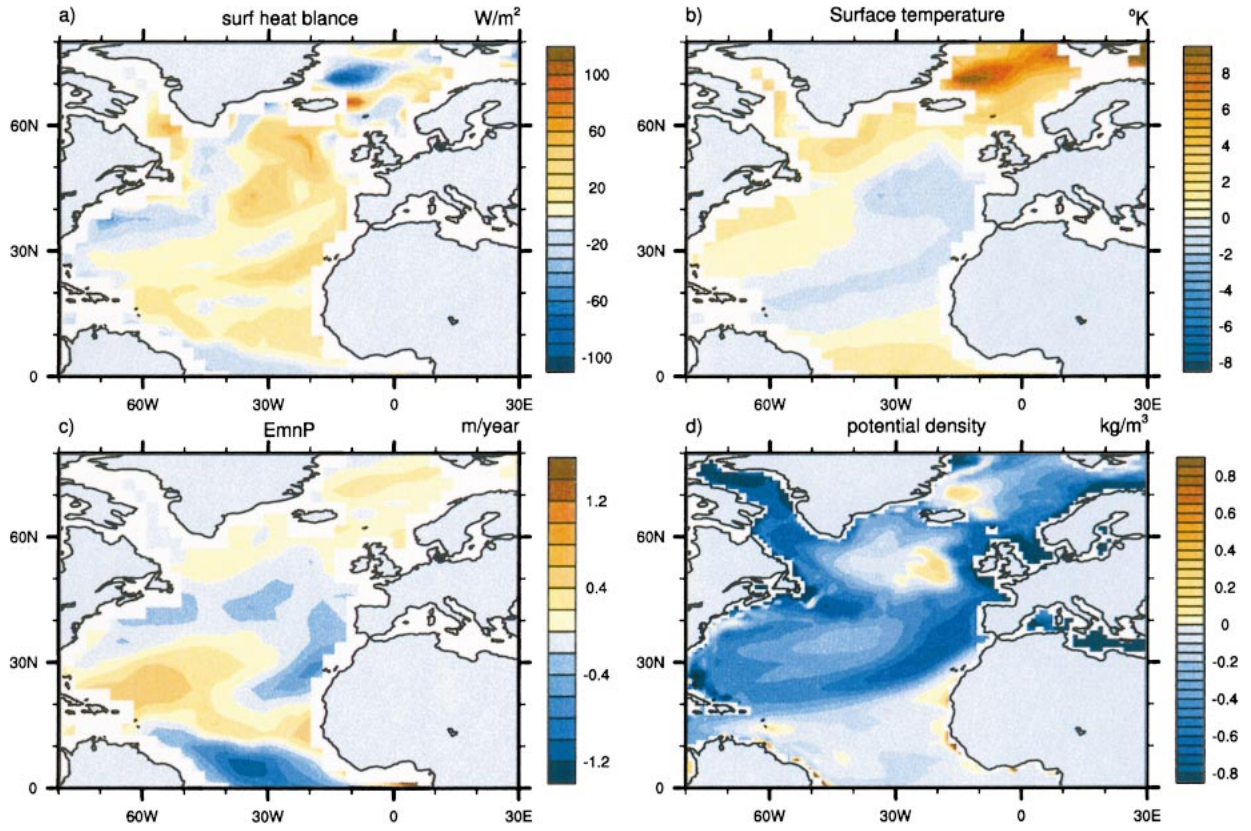

FIG. 8. Control run differences, CCSM minus PCTM, for North Atlantic (a) net surface energy balance (W m^{-2}), (b) SST (°C), (c) $E - P$ (m yr^{-1}), and (d) potential density of the ocean surface layer (kg m^{-3}).

itive values of $E - P$, as indicated by the negative upper ocean (top 300 m) density differences of about -0.2 to -0.4 kg m^{-3} over most of the North Atlantic in Fig. 8d. That is, the CCSM surface layer is less dense than PCTM, the ocean is more stable in the North Atlantic overall, and the MOC is reduced by 36% in CCSM compared to PCTM, all as the result of changing the atmospheric model.

Following the Raper et al. argument, the model with the greatest weakening of MOC should have the greatest ocean heat uptake efficiency. However, due to the results above, the change in base state MOC strength is a notable aspect of these simulations, and the percent change of MOC is a better indicator for these four models. Indeed, Fig. 7c shows that for the two most directly comparable models in terms of similar ocean and sea ice and different atmosphere, the PCTM and CCSM, the CCSM has the greater percent decrease of MOC of -7.3%, compared to the PCTM of -6.2%. For the PCM compared to PCTM, a different ocean but the same atmosphere produces a larger decrease of MOC of -9.9% for PCM compared to -6.2% for PCTM. This also results in a relative increase of ocean heat uptake in PCM compared to PCTM (Fig. 5b) and a slightly larger TCR (Fig. 4a). However, the model–dependent aspects that complicate the conclusions of Raper et al. regarding the apparent relationship between high k and low λ is shown dramatically for the CSM, where it has the lowest ocean heat uptake efficiency of all the models of 0.61°, but the lowest value of λ of 1.80 W m^{-2} $°C^{-1}$ and highest sensitivity with a TCR of 1.47°C (Fig. 4a). As noted above, the caveat that must accompany this analysis is that the four models considered here all have relatively small values of TCR and low sensitivity. The models surveyed by Raper et al. span a much larger sensitivity range, with the high sensitivity models showing the greatest decreases of MOC and largest k. Therefore, the generalizations of Raper et al. may apply across models with large variations of TCR, while the results here identify nuances of model-dependent processes that act among a class of low sensitivity models.

The net result of comparing the various factors contributing to k in Fig. 5b for the present four low sensitivity models indicates that the results are indeed highly model dependent, and relate directly to the combination of changes in MOC, high-latitude warming, and the relative contributions to the density change of temperature and salinity in the respective control runs and increased CO_2 simulations. Figure 5b is then consistent with the results in Fig. 4 in that the model with the most different atmosphere, the CCSM, has the most different value of ocean heat uptake.

Results shown here indicate that characteristics in the atmospheric model can affect how the ocean takes up heat, both in the control cases and in the increased CO_2 experiments. The consequence for the CCSM is that the ocean is more efficient in absorbing heat. This contributes to the lower TCR in CCSM compared to the other models, as well as a lower TCR even when equilibrium sensitivity is comparable with the other models. This points again to the importance of the atmospheric model for the coupled climate system response. However, the comparison of percent change of MOC with increased CO_2 between PCM compared to PCTM where only the ocean was changed, and PCTM compared to CCSM where only the atmosphere was changed, is consistent with the Raper et al. result that greater ocean heat uptake efficiency is associated with a relatively larger percent reduction in the strength of MOC. However, in contrast to the Raper et al. results, various combinations of model components can produce either larger ocean heat uptake efficiency associated with greater sensitivity (larger TCR), or larger ocean heat uptake efficiency associated with less sensitivity (smaller TCR).

Another interpretation of this result is that ocean heat uptake efficiency can be an active contributor to climate sensitivity. That is, greater ocean heat uptake means less heat available to warm the atmosphere, as is the case for CCSM, or less ocean heat uptake means that there is more heat to warm the atmosphere as for CSM. Conversely, it could be a passive reaction to the atmospheric response (greater ocean heat uptake means more heat is being forced into the ocean by a highly reactive atmosphere, as in the Raper et al. results).

6. Conclusions

Comparison among four global coupled climate models with various combinations of components, some in common but some different, supports the hypothesis that, to a greater degree than the other components, the atmospheric model ''manages'' relevant dynamically coupled *global* feedbacks including sea ice–albedo, water vapor, and clouds as well as characteristics of meridional overturning circulation in the ocean and ocean heat uptake efficiency. However, these responses must be studied in the fully coupled configuration since the atmospheric components among all models have comparable equilibrium climate sensitivities when coupled only to a slab ocean. This result points to the importance of feedbacks and ocean heat uptake in the coupled climate system. It also leads to the conclusion that, for global-scale dynamically coupled feedbacks, ocean, sea ice, and land surface do not play as important a role in the climate system response to increasing CO_2 as the atmosphere. However, regional temperature differences indicate that these components can be very important for the climate response on those spatial scales.

Two models with the same atmosphere and sea ice components but different ocean (PCM and PCTM) have the most similar response to increasing CO_2, followed closely by CSM with the same atmosphere and different ocean and sea ice from either PCM or PCTM. The CCSM has a different response from either of the other three, and in particular is different from PCTM in spite of the same ocean and sea ice but different atmospheric model components. Ocean heat uptake efficiency is shown to depend on the specific characteristics of the atmosphere in particular, with a change in the atmospheric model (from PCTM to CCSM) reducing not only the strength of the MOC in the control run, but also affecting the heat uptake efficiency with increased CO_2. That is, the CCSM, with the lowest climate sensitivity, has a somewhat greater percentage reduction of MOC compared to the PCTM. However, the CSM has a slight strengthening of MOC, greater high-latitude warming, but less heat uptake efficiency. Therefore, the nature of the climate system response to an input of increased energy to the system from increased CO_2 can be partitioned in various ways between atmosphere and ocean, with the nature of that partitioning related to the specific characteristics of the feedbacks in the system and the ocean heat uptake.

Acknowledgments. A portion of this study was supported by the Office of Biological and Environmental Research, U.S. Department of Energy, as part of its Climate Change Prediction Program, as well as the National Science Foundation.

REFERENCES

Boer, G. J., and B. Yu, 2003a: Dynamical aspects of climate sensitivity. *Geophys. Res. Lett.,* **30**, 1135, doi:10.1029/2002GL016549.

——, and ——, 2003b: Climate sensitivity and response. *Climate Dyn.,* **20,** 415–429.

Bonan, G. B., 1998: The land surface climatology of the NCAR land surface model (LSM 1.0) coupled to the NCAR Community Climate Model (CCM3). *J. Climate,* **11,** 1307–1326.

——, K. W. Oleson, M. Vertenstein, S. Levis, X. Zeng, Y. Dai, R. E. Dickinson, and Z.-L. Yang, 2002: The land surface climatology of the community land model coupled to the NCAR Community Climate Model. *J. Climate,* **15,** 3123–3149.

Cubasch, U., and Coauthors, 2001: Projections of future climate change. *Climate Change 2001: The Scientific Basis.* J. T. Houghton et al., Eds., Cambridge University Press, 525–582.

Dai, A., A. Hu, G. A. Meehl, W. G. Strand, and W. M. Washington, 2004: North Atlantic Ocean circulation changes in a millennial control run and projected future climates. *J. Climate,* submitted.

Dickinson, R. E., G. A. Meehl, and W. M. Washington, 1987: Ice-albedo feedback in a CO_2 doubling simulation. *Climatic Change,* **10,** 241–248.

Gent, P. R., 2001: Will the North Atlantic thermohaline circulation weaken during the 21st century? *Geophys. Res. Lett.,* **28,** 1023–1026.

——, F. Bryan, G. Danabasoglu, S. Doney, W. Holland, W. Large, and J. McWilliams, 1998: The NCAR Climate System Model global ocean component. *J. Climate,* **11,** 1287–1306.

——, A. P. Craig, C. M. Bitz, and J. W. Weatherly, 2002: Parameterization improvements in an eddy-permitting ocean model for climate. *J. Climate,* **15,** 1447–1459.

Gregory, J. M., and J. F. B. Mitchell, 1997: The climate response to

CO_2 of the Hadley Centre coupled AOGCM with and without flux adjustment. *Geophys. Res. Lett.,* **24,** 1943–1946.

Guilyardi, E., and Coauthors, 2004: Representing El Niño in coupled ocean–atmosphere GCMs: The dominant role of the atmosphere model. *J. Climate,* submitted.

Hu, A., G. A. Meehl, W. M. Washington, and A. Dai, 2004: Response of the Atlantic thermohaline circulation to increased atmospheric CO_2 in a coupled model. *J. Climate,* submitted.

Kiehl, J. T., J. J. Hack, G. Bonan, B. Boville, D. Williamson, and P. Rasch, 1998: The National Center for Atmospheric Research Community Climate Model (CCM3). *J. Climate,* **11,** 1131–1149.

Meehl, G. A., and W. M. Washington, 1990: CO_2 climate sensitivity and snow–sea-ice albedo parameterization in an atmospheric GCM coupled to a mixed-layer ocean model. *Climatic Change,* **16,** 283–306.

——, J. M. Arblaster, and W. G. Strand, 2000a: Sea ice effects on climate model sensitivity and low frequency variability. *Climate Dyn.,* **16,** 257–271.

——, W. D. Collins, B. Boville, J. T. Kiehl, T. M. L. Wigley, and J. M. Arblaster, 2000b: Response of the NCAR Climate System Model to increased CO_2 and the role of physical processes. *J. Climate,* **13,** 1879–1898.

——, P. Gent, J. M. Arblaster, B. Otto-Bliesner, E. Brady, and A. Craig, 2001: Factors that affect amplitude of El Niño in global coupled climate models. *Climate Dyn.,* **17,** 515–526.

Pacanowski, R. C., and S. G. H. Philander, 1981: Parameterization of vertical mixing in numerical models of the tropical oceans. *J. Phys. Oceanogr,* **11,** 1443–1451.

Ramanathan, V., and W. Collins, 1991: Thermodynamic regulation of ocean warming by cirrus clouds deduced from observations of the 1987 El Niño. *Nature,* **351,** 27–32.

Raper, S. C. B., J. M. Gregory, and R. J. Stouffer, 2002: The role of climate sensitivity and ocean heat uptake on AOGCM transient temperature response. *J. Climate,* **15,** 124–130.

Schneider, E. K., B. P. Kirtman, and R. S. Lindzen, 1999: Tropospheric water vapor and climate sensitivity. *J. Atmos. Sci.,* **56,** 1649–1658.

Spelman, M. J., and S. Manabe, 1984: Influence of oceanic heat transport upon the sensitivity of a model climate. *J. Geophys. Res.,* **89,** 571–586.

Stocker, T. F., and Coauthors, 2001: Physical climate processes and feedbacks. *Climate Change 2001: The Scientific Basis* (Contribution of Working Group I to the Third Assessment Report of the Intergovernmental Panel on Climate Change). J. T. Houghton et al., Eds., Cambridge University Press, 417–470.

Washington, W. M., and G. A. Meehl, 1989: Climate sensitivity due to increased CO_2: Experiments with a coupled atmosphere and ocean general circulation model. *Climate Dyn.,* **4,** 1–38.

——, and ——, 1991: Characteristics of coupled atmosphere–ocean CO_2 sensitivity experiments with different ocean formulations. *Greenhouse-Gas-Induced Climatic Change: A Critical Appraisal of Simulations and Observations,* M. E. Schlesinger, Ed., Elsevier, 79–110.

——, and Coauthors, 2000: Parallel climate model (PCM) control and transient simulations. *Climate Dyn.,* **16,** 755–774.